

UV EMISSION AND DUST PROPERTIES OF HIGH REDSHIFT GALAXIES

D. CALZETTI

*Space Telescope Science Institute
3700 San Martin Dr., Baltimore, MD 21218, U.S.A.*

Abstract. The high-redshift ($z > 2$) galaxies discovered over the last few years with the Lyman-break technique represent, in number density, a major fraction of the galaxies known in the Local Universe. Thus, understanding the properties and the nature of these high-redshift systems is instrumental to our understanding of the cosmic evolution of galaxies and their stellar content. I briefly review the observed characteristics of the Lyman-break galaxies, relate these galaxies to their most likely low-redshift counterparts, and discuss the implications of dust obscuration on the global properties of the Lyman-break population. Finally, the observational properties of the high-redshift population are set in the framework of a simple evolutionary model for the stellar, metal and dust content of galaxies, to derive the *intrinsic* star formation history of the Universe.

1. Introduction

Although this Meeting is devoted to the discussion of the nature of the Ultraluminous Far-IR Galaxies at low and high redshift, and their role in galaxy evolution, I will not directly tackle this topic in my presentation. I will instead summarize and discuss the properties of a complementary sample of galaxies: the high- z ($z > 2$), *UV-bright* systems ([30], [31]). The number of known $z > 2$ galaxies is now large enough that they can be classified as a *population*, and have been used to infer the past star formation history of the Universe ([22], [23]). As with all statistical studies, observational incompleteness and selection biases are a concern. In the case of the high- z population, volume corrections, luminosity selections and, last but potentially the most important, dust obscuration effects have been discussed by a number of authors (e.g., [24], [3], [27], [31], [5]). Here I will highlight the

impact of dust obscuration on the high- z galaxies and the inferred star formation history. I hope in this way to set a ground for comparison of the high- z UV-bright galaxy population with the high- z Ultraluminous Far-IR galaxies recently discovered with SCUBA ([28], [17], [2], [10]; see also the contributions of I. Smail, of A. Blain, and of M. Rowan-Robinson to these Proceedings).

2. The Lyman-Break Galaxies and their Low-Redshift Counterparts

Since it first was presented ([29]), the Lyman-break technique had stood out as one of the most powerful tools for identifying high- z galaxy candidates. As of this writing, more than 550 candidates have been spectroscopically confirmed to be at $z\sim 3$ over an area ~ 0.3 square degrees and about 50 at $z\sim 4$ over an area ~ 0.23 square degrees ([31]). In number density, the bright ends of the $z\sim 3$ and $z\sim 4$ populations have similar values to the local $L>L^*$ galaxies, for a flat cosmology. Even if merging may have played a role in changing these values over time, just the number of stars contained in Lyman-break galaxies at $z>2$ accounts for $\sim 20\text{--}30\%$ of all the stars known today. The basic fact is that the Lyman-break galaxy populations are a significant fraction of the total galaxy population today. Thus, understanding the nature of the Lyman-break galaxies remains a gateway to understanding the evolution of galaxies.

The identification of high- z candidates is based on the detection of the Lyman break at 912 \AA , which is the strongest discontinuity in the stellar continuum of star-forming galaxies. A galaxy at, say, $z=3$ will have the Lyman break redshifted to 3648 \AA . If a pair of filters is chosen to straddle the break, the galaxy will appear extremely red in this color. In order to avoid as much as possible low- z interlopers, one or more filters are generally added longward of the Lyman break to select only candidates which are blue in this(these) additional color(s). With a careful selection of the color criteria, the Lyman-break technique is extremely successful at identifying high- z candidates; spectroscopic confirmations give a $\sim 95\%$ success rate for the $z\sim 3$ sample and a $\sim 80\%$ success rate for the $z\sim 4$ sample ([30], [8], [31]). The lower success rate at $z\sim 4$ is due to the incidence of low- z interlopers, namely elliptical galaxies at $z\sim 0.5\text{--}1$ whose $4,000 \text{ \AA}$ break falls inside the selection window of the filters.

While the determination of the intrinsic nature of the Lyman-break galaxies, whether they are massive systems or galaxy fragments, and what kind of progenitors they are, is still a source of heated debate (e.g., [21], [13], [1]), the identification of their *observational* low- z counterparts appears less controversial.

By selection, Lyman-break galaxies are UV-bright, actively star-forming systems, with a preferentially blue spectral energy distribution (SED). Observed star formation rates (SFRs) range from a few to $50 M_{\odot} \text{ yr}^{-1}$, for a Salpeter Initial Mass Function (IMF) in the range $0.1\text{--}100 M_{\odot}$ ([8]). This range of values is typical of what observed in Local, UV-bright starburst galaxies (e.g., [4]). The restframe UV and B-band half-light radii are around $0.2\text{--}0.3$ arcsec, which correspond to spatial radii $\sim 1\text{--}3 h_{50}^{-1}$ kpc, depending on q_o ([12], [14]). The similarity of the half-light radii at both UV and B suggests that the UV is a reliable tracer of the full extent of the light-emitting body. Ground-based optical spectra, which correspond to the restframe $900\text{--}1800 \text{ \AA}$ range for a $z\sim 3$ galaxy, show a wealth of absorption features, and sometime P-Cygni profiles in the CIV(1550 \AA) line (cf. the figures in [30]), typical of the predominance of young, massive stars in the UV spectrum. Currently limited ground-based near-IR spectroscopy (e.g. [27]) has revealed nebular line emission in these galaxies. Hybrid line equivalent widths constructed using the UV flux density $f(\text{UV})$ as denominator, namely, $\text{EW}'(\text{\AA}) = F(\text{line})/f(\text{UV})$, show that the observed values for the high- z galaxies fall in the loci observed for local starburst galaxies ([25]). In summary, *the observational properties of the Lyman-break galaxy population fully resemble, in the restframe UV-optical range, those of low-redshift, UV-bright starburst galaxies* ([25]).

The Lyman-break galaxies share another global characteristic with the Local starbursts. If we parametrize the observed UV stellar continuum with a power law, $F(\lambda) \propto \lambda^{\beta}$, Lyman-break galaxies cover a large range of β values, roughly from -3 to 0.4 , namely from very blue to moderately red (Figure 1, left panel). This range is not very different from that covered by the Local, UV-bright starbursts (Figure 1, right panel). Population synthesis models (e.g. [19]) indicate that a dust-free, young starburst or constant star-formation population have invariably values of $\beta < -2.0$, for a vast range of metallicities. *What does cause the UV stellar continuum of Lyman-break galaxies to be redder than expected for a young star-forming population?*

3. Dust Reddening and Obscuration in Local Starbursts and in Lyman-break Galaxies

There are two main causes for a red UV stellar continuum: 1) ageing of the stellar population; 2) presence of dust (variations of the intrinsic IMF will not be discussed here).

An ageing stellar population loses the high-mass, hot stars first, and then, progressively, lower-mass and colder stars. In the process, the UV stellar continuum becomes redder and redder and, also, the $4,000 \text{ \AA}$ break

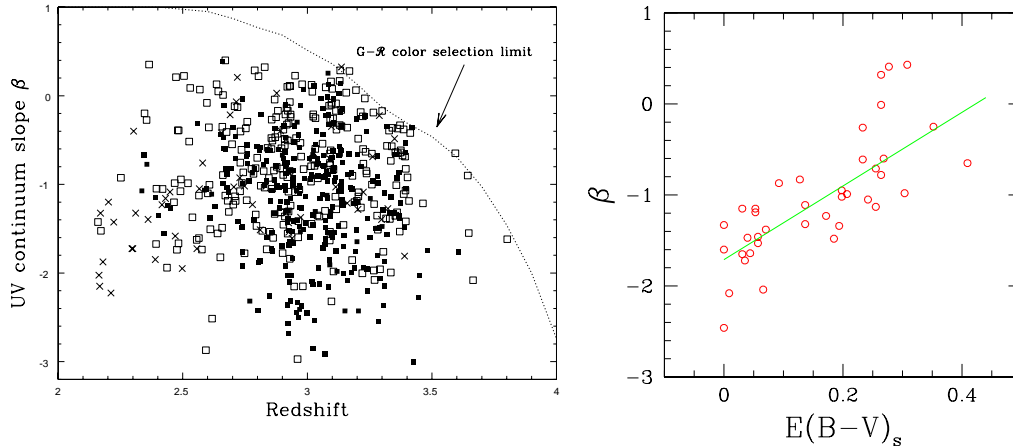


Figure 1. (Left Panel) The distribution of the observed UV spectral indices β of the $z \approx 3$ galaxies (M. Dickinson 1998, private communication). Only a small fraction of all the galaxies are blue enough ($\beta < -2$) to be classifiable as dust-free, young star-forming populations. Different symbols corresponds to different color selections. (Right Panel) The distribution of β for a UV-bright sample of Local starburst galaxies ([18]). Note that the range of β values is similar to the high- z sample. The UV spectral slopes of the local starbursts correlate with $E_s(B-V)$, the color excess of the optical stellar continuum due to dust reddening ([6], [4]). Blue UV spectra correspond to small values of the color excess, red UV spectra to large values of $E_s(B-V)$. The best fit line through the data is shown.

increases in strength. This break spans a small wavelength range, thus is unaffected by dust reddening. The strength of the $4,000 \text{ \AA}$ break is therefore a powerful constraint on the age of the stellar population. The Local starbursts can have very red UV continua ($\beta > 0$), while still showing rather small $4,000 \text{ \AA}$ breaks, telltales of the presence of a young stellar population ($< 10^7$ yr) or of constant star formation (over timescales $\sim 10^9$ yr, see [4]). Ageing of the stellar population is not the main reason for the presence of a red UV SED in Local starbursts. Broad-band J, H, and K observations provide limited information on the strength of the $4,000 \text{ \AA}$ break in high- z galaxies, still accurate enough to exclude ageing as a general cause for the red UV spectra in this case as well (Dickinson 1997, priv. communication).

Dust reddening is then the likely cause for red UV spectra, as demonstrated by the correlation between β and color excess (Figure 1, right panel). Dust reddening is generally a close-to-unsolvable problem for unresolved stellar populations (e.g., distant galaxies), because the effective obscuration will be a combination of dust distribution relative to the emitters, scattering, and environment-dependence of the extinction ([33], [6]). The situation gets better in the case of starbursts because the high energy environment is generally inhospitable to dust. Shocks from supernovae can

destroy dust grains, while gas outflows can eject significant amounts of interstellar gas and dust from the site of star formation. If little diffuse dust is present within the star-forming region, the main source of opacity will come from the dust surrounding the region. Parametrizing the ‘net’ obscuration of the stellar continuum as: $F_{obs}(\lambda) = F_0(\lambda) 10^{-0.4E_s(B-V) k(\lambda)}$, with $F_{obs}(\lambda)$ and $F_0(\lambda)$ the observed and intrinsic fluxes, respectively, obscuration in starbursts is expressed as:

$$\begin{aligned} k(\lambda) &= 2.656(-2.310 + 1.315/\lambda) + 4.88 & 0.63 \mu m \leq \lambda \leq 1.60 \mu m \\ &= 2.656(-2.156 + 1.509/\lambda - 0.198/\lambda^2 + 0.011/\lambda^3) + 4.88 \\ && 0.12 \mu m \leq \lambda < 0.63 \mu m. \end{aligned} \quad (1)$$

The connection between the color excess $E_s(B-V)$ and the measured spectral slope β is given by the correlation in Figure 1 (right panel).

It is worth stressing that, although dust reddening corrections for starbursts are parametrized above as a foreground dust screen, *Equation 1 has been derived with NO assumptions on the geometrical distribution of the dust within the galaxies.* Equation 1 is a purely empirical result ([6], [4]), which includes into a single expression any effect of dust geometry, scattering, and environment-dependence of the dust composition.

Equation 1 provides a recipe for correcting the observed SEDs for the effects of dust reddening. Does it fully account for the dust obscuration as well? In other words, does Equation 1 completely recover the light from the region of star formation or does it miss the flux from dust-enshrouded regions? The answer to these questions is a positive one: Equation 1 is able to recover, within a factor ~ 2 , the UV-optical light from the entire star-forming region of *UV-bright*, i.e. moderately obscured, starbursts.

We can prove the above statement by studying the FIR emission of the local starbursts. Dust emits in the Far-IR the stellar energy absorbed in the UV-optical. However, the Far-IR emission is not, by itself, an unambiguous measure of the opacity of the galaxy, as the intensity of the dust emission is also a function of the SFR in the galaxy. A good measure of the total opacity of the galaxy is instead provided by the ratio FIR/F(UV) ([25]). The Far-IR flux, FIR, and the UV flux, F(UV), are both proportional to the SFR, but their sensitivity to dust has opposite trends: roughly, FIR increases while F(UV) decreases for increasing amounts of dust, although the details of the trends are dictated by the geometrical distribution of the dust. In the assumption that the foreground dust screen parametrization is valid, the FIR/F(UV) ratio is related to the UV attenuation in magnitudes, $A(UV)$, via ([25]):

$$FIR/F(UV) = 1.19 \left[10^{0.4A(UV)} - 1 \right], \quad (2)$$

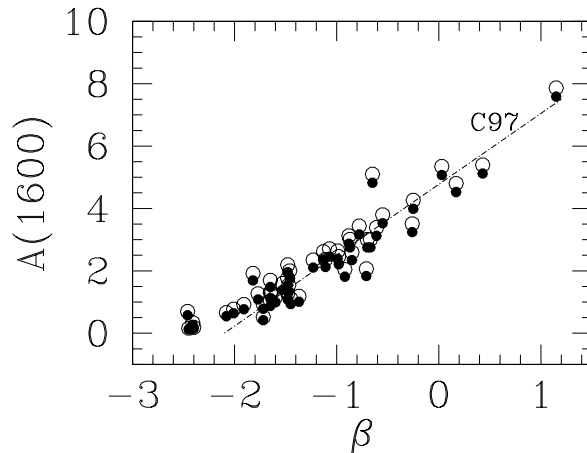


Figure 2. The attenuation in magnitudes at 1,600 Å, $A(1600)$, as a function of the UV spectral index β . The data points (empty and filled circles) are from the same sample of UV-bright, local starbursts of Figure 1 ([18]). $A(1,600)$ is proportional to $\log[FIR/F(UV)]$ where FIR and $F(UV)$ are the Far-IR and UV observed luminosities, respectively (see text). The filled and empty circles correspond to two different choices of the bolometric-to-FIR correction for the dust emission. This is the most uncertain parameter in the derivation of Equation 2; yet, its effect on the data is fairly small. The straight line across the data, marked C97, is the location of the reddening curve of Equation 1, with $\beta_0 = -2.1$ for $E_s(B-V)=0$ ([4]). There are no adjustable parameters in the positioning of the C97 line. The agreement between the data points and the predicted attenuations from the reddening curve (Equation 1) demonstrates that reddening corrections can fully recover the intrinsic UV emission from these galaxies and the amount of star formation buried in dust is relatively small.

where the constant value 1.19 is the combination of the ratio of the bolometric stellar luminosity to the UV luminosity and the ratio of the bolometric dust emission to the FIR emission. Since $F(UV)$ and FIR (e.g., from IRAS) are measurable in galaxies, as is β , the UV attenuation can be related to the UV spectral slope via Equation 2 ([25]). Figure 2 shows $A(UV)$ measured at 1,600 Å as a function of β for a sample of Local starbursts. Overplot on the data is the trend predicted by Equation 1, with β related to $E_s(B-V)$ using Figure 1 and the limiting case $\beta_0 = -2.1$ for $E_s(B-V)=0$ ([4]). Equation 1 and Figure 1 have no adjustable parameters. The agreement between the data and the predicted trend is therefore impressive, especially if we take into account that the latter is a recipe for *reddening*, and could in principle not account for the entire dust obscuration. Discrepancies at the low end of the locus of data points in Figure 2 are understandable in terms of sample incompleteness.

How does all this apply to Lyman-break galaxies? The entire purpose of obtaining dust obscuration corrections for the high- z galaxy sample is

to recover the intrinsic UV emission of the galaxies, therefore deriving a more meaningful UV luminosity function, a more accurate value of the SFR for each object (which can bear into the understanding of the nature of these objects), and, finally, the *intrinsic* cosmic SFR density ([22]). Figure 1 (right panel) shows the observed UV spectral slopes of the $z\sim 3$ galaxies. Those slopes can be ‘translated’ into a value of the effective color excess, which is calculated to have mean value $E_s(B-V)\simeq 0.15$ for the $z\sim 3$ galaxies, or an attenuation $A(1600)\simeq 1.6$ mag ([31], see also [3]). Incidentally, this mean value of $E_s(B-V)$ is similar to that observed in the local starburst sample ([3]); this is purely coincidental, and is borne of the fact that the two samples of galaxies cover similar ranges of β . A similar mean value of the effective color excess has been obtained by Pettini et al. ([27]) from the analysis of the nebular emission lines in the NIR spectra of a small sample of Lyman-break galaxies. Correcting the observed UV spectra for dust attenuation increases the median SFR of $\approx \times 5$ in the $z>2$ galaxies and of $\approx \times 3$ in the $z\leq 1$ galaxies (Figure 3). The difference in the correction factors at low and high- z is entirely due to the different wavelengths at which the two redshift regimes are probed: $\sim 1,600$ Å the high- z galaxies and $\sim 2,800$ Å the lower- z galaxies. The dust correction factors have been ‘measured’ only for the high- z sample and have been assumed to hold unchanged for the $z\leq 1$ sample, modulo the change in wavelength (see discussion in [31]).

4. The Evolution of the Stellar, Metal, and Dust Content of Galaxies

The next question in line is whether a median attenuation of ~ 1.6 mag in the UV is reasonable at $z > 2$, when galaxies were at most a few Gyr old and, presumably, metal- and dust-poor. Both the Cosmic Far-IR Background (CIB) detected by COBE ([11], [16]) and the FIR-bright galaxies detected by SCUBA at $z\geq 1$ ([28], [17], [2], [10]) demonstrate that dust was present at high redshift. The luminosity of the CIB is about 2.5 times higher than the luminosity of the UV-optical Background ([23]), implying a proportionally higher contribution of the redshift-integrated dust emission. However, neither the CIB nor the SCUBA galaxies are telling us how the dust content in galaxies has evolved with redshift. In the case of the SCUBA galaxies, the redshift and luminosity distribution and the AGN fraction of the sources will need to be tackled before providing such information.

The time evolution of the UV luminosity density of galaxies and of the derivative SFR density (Figure 3) can be used to constrain the metal and dust enrichment of galaxies and, therefore, the intrinsic SFR density ([5]). The stars which produce the observed UV luminosity at each redshift pro-

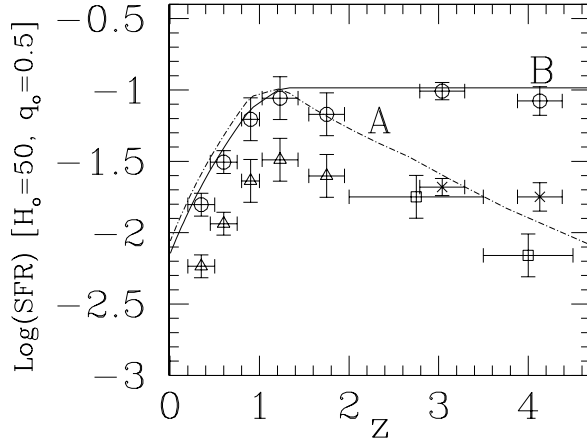


Figure 3. The SFR density, in $M_{\odot} \text{ yr}^{-1} \text{ Mpc}^{-3}$, as a function of redshift z . The data points are derived from the UV luminosity density of galaxies, converted to SFR using a Salpeter IMF in the range 0.35–100 M_{\odot} and continuous SF. The triangles are the observed values at 2,800 \AA of Lilly et al. ([20]) and Connolly et al. ([7]). The squares are the observed values at $\sim 1,600 \text{\AA}$ as reported in Madau et al. ([23]), while the crosses are the new values from the Lyman-break galaxies by Steidel et al. ([31]). The circles represent the *intrinsic* SFR densities from the data of Lilly et al., Connolly et al., and Steidel et al., *corrected for dust obscuration* using $E_s(B-V)=0.15$ (see [31]). The curves marked A and B bracket the range of solutions for the *intrinsic SFR density* from the evolution model described in Section 4. Curve B agrees well with the obscuration-corrected data points (circles).

duce also metals and dust with negligible delay times, at most 100-200 Myr in the case of dust ([9]). The obscuration from dust will produce an *observed* UV flux lower than the true flux. Once the effects of the dust on the observed UV emission are evaluated and removed, a new SFR density is calculated. The procedure is repeated iteratively till convergence ([5]). A number of observational constraints are used in the model: no more than $\sim 10\%$ of the baryons are in galaxies; inflows/outflows keep the $z=0$ metallicity of the gas in galaxies to about solar, with a $\sim 15\%$ mean residual gas content, and the $z\sim 2-3$ metallicity to about 1/10–1/15 solar ([26]); the intrinsic SFR density at $z=0$ must be comparable with that measured from $H\alpha$ surveys ([15]); the dust emission must reproduce the observed CIB and not exceed the FIR emission of local galaxies.

These constraints are still not enough to yield a unique solution; one of the missing ingredients is the behavior of the SFR density at $z>4$, where there are no data points. Different assumptions will lead to different intrinsic SFR histories. The range of solutions is bracketed by Models A and B in Figure 3. Figure 4 shows, for each of the two solutions, the evolution of the dust column density in the average galaxy and the contribution to the

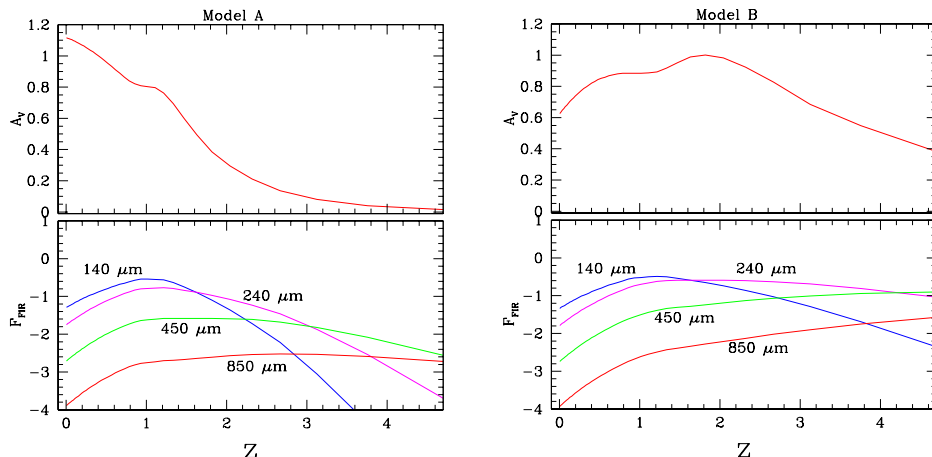


Figure 4. The evolution of the dust column density in galaxies (top panels), expressed as optical attenuation A_V in magnitudes, and of the contribution to the CIB at selected wavelengths (bottom panels) as a function of redshift, for both Model A (left panels) and Model B (right panels). Models A and B are the intrinsic SFR densities described in Figure 3 and Section 4. For both models the dust optical depth remains relatively modest at all redshifts. Yet, this is sufficient to fully account for the CIB luminosity. The contributing flux to the CIB is shown at the observer’s restframe wavelengths 140 μm , 240 μm , 450 μm , and 850 μm , in arbitrary units. The two models predict different mean redshifts for the main contributors at each wavelength. In theory, this difference could be used to discriminate between the two solutions. However, some caution should be used as the spectral shape of the CIB is quite dependent on the dust emission SED adopted for the individual galaxies (in our case a single temperature blackbody combined with a ν^2 emissivity model).

CIB at selected wavelengths as a function of redshift. The latter is however dependent on the assumptions about the intrinsic dust emission SED, which is not well constrained.

Model B resembles the SFR density derived from the obscuration corrected Lyman-break galaxies (Figure 3). This demonstrates that attenuations of about 1.6 mag in the UV are perfectly reasonable within the framework of a simple model of stellar and dust content evolution in galaxies.

5. The Intrinsic Star Formation History of the Universe and the SCUBA galaxies

The shape of Model B resembles the SFR history expected for the ‘monolithic collapse’ model of galaxy evolution, although expectations for hierarchical galaxy formation models are not ruled out ([32], see discussion in [31]; see also the contribution of G. Kauffmann to these Proceedings). Thus the monolithic-versus-hierarchical dilemma is still unsolved by our current

knowledge of the SFR history. Values of the SFR density at higher redshifts ($z \geq 5$) will be able place more definite constraints on the galaxy evolution scenario.

The final question we want to ask is what fraction of the total SFR density the Lyman-break galaxies represent at each given redshift. And how much of the SF is so deeply buried in dust that its accounting is missing. The obscuration curve discussed in Section 3 is technically valid only for UV-bright star-forming galaxies; it cannot, obviously, correct for objects which are missing from the sample because they are too dusty. On the one hand, Model B is only slightly in excess of the obscuration-corrected SFR density calculated from the $z > 2$ galaxies (by a negligible amount within the observational uncertainties), and the SFR history of Model B is perfectly sufficient to reproduce the observed CIB. It appears that the fraction of SF missed by considering the Lyman-break galaxies only is relatively small. On the other hand, a number of considerations invite to take this as a preliminary statement. We know that at low redshift a fraction of the star formation is deeply buried in dust, and is obscured even at IR wavelengths. The same could happen at high redshift, and the SCUBA sources seem to suggest that large dust contents are not impossible in high- z galaxies. The angular density of the SCUBA sources is about 1/2–1 of that of the $z \sim 3$ galaxies, and are spread over a (possibly) much larger redshift range than the Lyman-break galaxies, namely over ~ 5 – $10 \times$ larger cosmological volumes. The SCUBA sources are then ~ 5 – 20% of the Lyman-break galaxies by number density, but are forming stars with $\text{SFR} \approx 300$ – $500 M_{\odot} \text{ yr}^{-1}$. Thus the SCUBA galaxies could still add ≈ 25 – 100% to the SFR density of the *obscuration-corrected* Lyman-break galaxies, although an assessment of the AGN contribution is still missing.

Because of their characteristics, the two populations, the UV-bright Lyman-break galaxies and the FIR-bright SCUBA sources, are likely to be complementary, rather than overlapping. At the level of current knowledge, it appears that about 50–80% of the SF in the early phases of the Universe is accounted for by the *obscuration-corrected* Lyman-break galaxies; the remaining 20–50% of the SF may be contained in FIR-bright sources. However, more investigation of the nature, luminosity distribution and redshift placement of the SCUBA sources is needed before these figures can be taken at face value.

ACKNOWLEDGEMENTS. I am indebted with C. Steidel, M. Giavalisco, and M. Dickinson for making their most recent results on the Lyman-break galaxies available to me prior to publication, for discussions, and for a critical reading of the manuscript. I would like to thank the Organizing Committee for inviting me to this stimulating meeting and for financially support my stay at the Ringberg Castle.

References

1. Adelberger, K.L., Steidel, C.C., Giavalisco, M., Dickinson, M.E., Pettini, M., & Kellogg, M. 1998, *ApJ*, 505, 18
2. Barger, A.J., Cowie, L.L., Sanders, D.B., Fulton, E., Taniguchi, Y., Sato, Y., Kawara, K. & Okuda, H. 1998, *Nature*, embargoed (astroph/9806317)
3. Calzetti, D. 1997a, in *The Ultraviolet Universe at Low and High Redshift: Probing the Progress of Galaxy Evolution*, eds. W.H. Waller, M.N. Fanelli, J.E. Hollis & A.C. Danks, *AIP Conf. Proc.* 408 (Woodbury: AIP), 403
4. Calzetti, D. 1997, *AJ* 113, 162
5. Calzetti, D., & Heckman, T.M. 1998, *ApJ*, in press (astroph/9811099)
6. Calzetti, D., Kinney, A.L., & Storchi-Bergmann, T. 1994, *ApJ*, 429, 582
7. Connolly, A.J., Szalay, A.S., Dickinson, M., Subbarao, M.U., & Brunner, R.J. 1997, *ApJ*, 486, L11
8. Dickinson, M. 1998, in *The Hubble Deep Field, STScI May Symposium*, eds. M. Livio, S.M. Fall, & P. Madau, (Cambridge: CUP), in press (astroph/9802064)
9. Dwek, E. 1998, *ApJ*, 501, 643
10. Eales, S., Lilly, S., Gear, W., Dunne, L., Bond, J.R., Hammer, F., Le Fèvre, O., & Crampton, D. 1998, *ApJ*, submitted (Letters)
11. Fixsen, D.J., Dwek, E., Mather, J.C., Bennett, C.L., Shafer, R.A. 1998, *ApJ*, in press (astroph/9803021)
12. Giavalisco, M., Steidel, C.C., & Macchetto, F.M. 1996, *ApJ*, 470, 189
13. Giavalisco, M., Steidel, C.C., Adelberger, K.L., Dickinson, M.E., Pettini, M., & Kellogg, M. 1998, *ApJ*, 503, 543
14. Giavalisco, M., et al. 1999, in prep.
15. Gronwall, C., 1998, in *Dwarf Galaxies and Cosmology, the XXXIIIrd Recontres de Moriond*, eds. T.X. Thuan, C. Balkowski, V. Cayatte & J. Tran Thanh Van (Gif-sur-Yvette: Editions Frontières), in press (astroph/9806240)
16. Hauser, M.G., et al. 1998, *ApJ*, in press (astroph/9806167)
17. Hughes, D., Serjeant, S., Dunlop, J., Rowan-Robinson, M., Blain, A., Mann, R.G., Ivison, R., Peacock, J., Efstathiou, A., Gear, W., Oliver, S., Lawrence, A., Longair, M., Goldschmidt, P., & Jenness, T. 1998, *Nature*, 394, 241
18. Kinney, A.L., Bohlin, R.C., Calzetti, D., Panagia, N., & Wyse, R.F.G. 1993, *ApJS*, 86, 5
19. Leitherer, C., & Heckman, T.M. 1995, *ApJS*, 96, 9
20. Lilly, S.J., Le Fèvre, O., Hammer, F. & Crampton, D. 1996, *ApJ*, 460, L1
21. Lowenthal, J., Koo, D., Guzman, R., Gallego, J., Phillips, A.C., Faber, S.M., Vogt, N.P., Illingworth, G.D., & Gronwall, C. 1997, *ApJ*, 481, 673
22. Madau, P., Ferguson, H.C., Dickinson, M.E., Giavalisco, M., Steidel, C.C., & Fruchter, A. 1996, *MNRAS*, 283, 1388
23. Madau, P., Pozzetti, L., & Dickinson, M. 1998, *ApJ*, 498, 106
24. Meurer, G. R., Heckman, T.M., Lehnert, M.D., Leitherer, C., & Lowenthal, J. 1997, *AJ*, 114, 54
25. Meurer, G. R., Heckman, T. M., & Calzetti, D. 1998, *ApJ*, submitted
26. Pettini, M., Smith, L.J., King, D.L., & Hunstead, R.W. 1997, *ApJ*, 486, 665
27. Pettini, M., Kellogg, M., Steidel, C.C., Dickinson, M., Adelberger, K.L., & Giavalisco, M. 1998, *ApJ*, in press (astroph/9806219)
28. Smail, I., Ivison, R.J., & Blain, A.W. 1997, *ApJ*, 490, L5
29. Steidel, C.C., & Hamilton, D. 1993, *AJ*, 105, 2017
30. Steidel, C.C., Giavalisco, M., Pettini, M., Dickinson, M., & Adelberger, K.L. 1996, *ApJ*, 462, L17
31. Steidel, C.C., Adelberger, K.L., Giavalisco, M., Dickinson, M., & Pettini, M. 1998, *ApJ*, submitted (astroph/9811399)
32. White, S.D.M., & Frenk, C.S. 1991, *ApJ*, 379, 25
33. Witt, A.N., Thronson, H.A., & Capuano, J.M. 1992, *ApJ*, 393, 611